HHS Public Access

Author manuscript

J Cell Biochem. Author manuscript; available in PMC 2017 April 01.

Published in final edited form as:

J Cell Biochem. 2016 April ; 117(4): 959–969. doi:10.1002/jcb.25380.

C-Mpl is expressed on osteoblasts and osteoclasts and is important in regulating skeletal homeostasis

Tomas E. Meijome[1,†], **Jenna T. Baughman**[1,†], **R. Adam Hooker**[1], **Ying-Hua Cheng**[1], **Wendy A. Ciovacco**[1,2], **Sanjeev M. Balamohan**[1], **Trishya L. Srinivasan**[1], **Brahmananda R. Chitteti**[3], **Pierre P. Eleniste**[4], **Mark C. Horowitz**[2], **Edward F. Srour**[3], **Angela Bruzzaniti**[4], **Robyn K. Fuchs**[5], and **Melissa A. Kacena**[1,2,*]

[1]Department of Orthopaedic Surgery, Indiana University School of Medicine, Indianapolis

[2]Department of Orthopaedics and Rehabilitation, Yale University School of Medicine, New Haven, CT

[3]Department of Medicine, Indiana University School of Medicine, Indianapolis

[4]Department of Oral Biology, Indiana University School of Dentistry, Indianapolis

[5]Department of Physical Therapy, Indiana University School of Health and Rehabilitation Sciences, Indianapolis

Abstract

C-Mpl is the receptor for thrombopoietin (TPO), the main megakaryocyte (MK) growth factor, and c-Mpl is believed to be expressed on cells of the hematopoietic lineage. As MKs have been shown to enhance bone formation, it may be expected that mice in which c-Mpl was globally knocked out (c-Mpl−/− mice) would have decreased bone mass because they have fewer MKs. Instead, c-Mpl−/− mice have a higher bone mass than WT controls. Using c-Mpl−/− mice we investigated the basis for this discrepancy and discovered that c-Mpl is expressed on both osteoblasts (OBs) and osteoclasts (OCs), an unexpected finding that prompted us to examine further how c-Mpl regulates bone. Static and dynamic bone histomorphometry parameters suggest that c-Mpl deficiency results in a high bone turnover state with a net gain in bone volume. In vitro, a higher percentage of c-Mpl −/− OBs were in active phases of the cell cycle, leading to an increased number of OBs. No difference in OB differentiation was observed in vitro as examined by real-time PCR and functional assays. In co-culture systems, which allow for the interaction between OBs and OC progenitors, c-Mpl−/− OBs enhanced osteoclastogenesis. Two of the major signaling pathways by which OBs regulate osteoclastogenesis, MCSF/OPG/RANKL and EphrinB2-EphB2/B4, were unaffected in c-Mpl−/− OBs. These data provide new findings for the role of MKs and c-Mpl expression in bone and may provide insight into the homeostatic regulation of bone mass as well as bone loss diseases such as osteoporosis.

[*]**Corresponding Author:** Melissa Kacena, Ph.D., August M. Watanabe Translational Scholar, Showalter Scholar, Associate Professor, Indiana University School of Medicine, Department of Orthopaedic Surgery, 1130 West Michigan St, FH 115, Indianapolis, IN 46202, (317) 278-3482 – phone, (317) 278-9568 – fax, ; Email: mkacena@iupui.edu

[†]Contributed equally to this work

The authors have no conflicts of interest.

Keywords

Thrombopoietin; c-Mpl; osteoblasts; osteoclasts; bone mass

INTRODUCTION

Traditionally, skeletal and hematopoietic systems have been studied as separate entities. However, given their shared site of origin in the bone marrow cavity, it is broadly accepted that the two cell lineages would have the ability to exert local influence on each other. A growing body of evidence suggests that MKs and/or their growth factors play a role in skeletal homeostasis. Indeed, our group and others have shown that increased levels of MKs lead to amplified OB proliferation and phenotypes displaying increased bone mass (Kacena et al.,2004; Kacena et al.,2012; Kacena et al.,2005; Miao et al.,2004; Cheng et al.,2013; Meijome et al.,2015; Cheng et al.,2015; Ciovacco et al.,2010; Lemieux et al.,2010; Ciovacco et al.,2009).

Specifically, our laboratory has previously shown that mice deficient in GATA-1 or NF-E2, transcription factors that are necessary for normal MK differentiation, develop a striking increase in bone marrow MK number with a concomitant reduction in platelet number and a dramatic increase in trabecular bone (Kacena et al.,2004; Shivdasani et al.,1995; Shivdasani et al.,1997). Similarly, overexpression of thrombopoietin (TPO), the major MK growth factor, in mice results in an approximate 4-fold increase in bone marrow MK number and an osteosclerotic bone phenotype (Villeval et al.,1997; Yan et al.,1996). Because of the similar increase in bone marrow MK number and high bone mass phenotype, we previously postulated TPO acts upon MKs and these MKs subsequently activate OB lineage cells, leading to an increase in bone formation. Based in part on this model, Perry et al examined whether a reduction in MK number would result in a reduction in bone (Perry et al.,2007). To do this they also examined mice deficient in c-Mpl, the receptor for TPO, which is thought to be highly restricted to hematopoietic stem cells and cells of the MK lineage. Although c-Mpl−/− mice have a significant reduction in MK numbers (>80% reduction) (de Sauvage et al.,1996), Perry et al found no difference in bone phenotype between c-Mpl−/− mice and wild-type (WT) controls (Perry et al.,2007) when a decrease in bone formation may have been expected.

Based on these apparently contradictory findings we examined potential mechanisms leading to increased bone mass in c-Mpl−/− mice and investigated new parameters including the direct effect of c-Mpl deletion on cells of the bone cell and the enumeration of numbers of OB and OC numbers in c-Mpl−/− mice. We report important new findings that cells of the OC and OB lineage express c-Mpl, and that c-Mpl expression can impact both OC and OB growth and function and may shed light on the direct and indirect effects of c-Mpl in regulating skeletal homeostasis.

METHODS

Mice

For these studies 5 month-old female and male c-Mpl−/− or knockout (on a C57BL/6 background) and wild-type (WT) C57BL/6 mice were utilized. C-Mpl knockout mice were kindly provided by Genentech. Generation and breeding of c-Mpl knockout mice was previously described (Gurney et al., 1994; Tong and Lodish, 2004; de Sauvage et al.,1994). C57BL/6 mice were obtained from Jackson Laboratories. Three and thirteen days prior to sacrifice, mice were injected with 30mg/kg of calcein (IP) for dynamic histomorphometric determinations. All procedures were approved by the Institutional Animal Care and Use Committee (IACUC) of the Indiana University School of Medicine and followed NIH guidelines as well as the Guide for the Care and Use of Laboratory Animals.

Histology/Histomorphometry

The WT and cMpl−/− mice were administered an intraperitioneal injection of the fluorochrome calcein (30mg/kg) 13 and 3 days prior to sacrifice to label actively forming bone surfaces. Static and dynamic histomorphometric analysis of trabecular bone was performed on femurs as previously described (Feher et al.,2010; Warden et al.,2008). Histological measurements were made with a semiautomatic analysis system (Bioquant OSTEO 7.20.10, Bioquant Image Analysis Co.) attached to a microscope with an ultraviolet light source (Nikon Optiphot 2 microscope, Nikon). Measurements were done on one stained (static) and one unstained (dynamic) section for each animal.

μCT

Micro-computed tomography or μCT (Skyscan 1172) was used to quantify trabecular bone parameters of the distal femur as previously detailed (Feher et al.,2010; Warden et al.,2008; Weatherholt et al.,2013). μCT scanning was performed on the femur sequestered for histology. In brief, images were binarized, and three-dimensional bone volume parameters were calculated: trabecular bone volume fraction (BV/TV, %), trabecular number (Tb.N, 1/mm), trabecular thickness (Tb.Th, mm), and trabecular separation (Tb.Sp, mm).

Biomechanics

Relative bone strength was determined by performing three-point bending of the left femur with a materials testing device (MTS Systems Corporation; Eden Prairie, MN) as previously detailed (Warden et al.,2008; Feher et al.,2010; Weatherholt et al.,2013). In brief, femurs were thawed to room temperature in a saline bath for two hours. Thereafter, each femur was tested in the anterior-posterior direction and stabilized with a static preload of 1 N before being loaded to failure with a crosshead speed of 10 mm/min. Force versus displacement data was gathered at 100 Hz, and the ultimate force (N), stiffness (N/mm), polar moment of inertia, ultimate stress (MPa), modulus (MPa), and toughness (MJ/m3) were derived.

Preparation of Neonatal Calvarial Cells (OB)

Neonatal murine calvarial OB cells were prepared as previously described (Horowitz et al., 1994) from WT C57BL/6 and c-Mpl −/− mice. Our technique was a modification of the

basic method described by Wong (Wong and Cohn, 1975). Briefly, calvaria were dissected from neonatal mice and then treated with EDTA in PBS for 30 min. Calvaria were then subjected to sequential collagenase digestions (200U/mL). Fractions 3–5 (digestions incubated at 37°C for 20–35, 35–50, and 50–65 min, respectively) were collected and used as the OB starting population. These cells were ~90% OB or OB precursors based on previously reported established criteria (Horowitz et al.,1994; Simmons et al.,1982; Jilka and Cohn, 1981). OBs were seeded at $2x10^4$ cells/ml (optimal pre-tested). OB in culture were maintained in αMEM supplemented with 10% fetal bovine serum and were further supplemented with ascorbic acid (50 μg/ml added on day 0 and at all feedings) and β-glycerophosphate (5mM added starting on day 7 and all subsequent feedings). Cells were fed twice per week. Thrombopoietin (TPO) was added to some cultures. Multiple doses of TPO were tested (1–1000 ng/ml) and none of these doses resulted in an appreciable difference in OB proliferation (data not shown). Therefore, we selected the TPO dosage our group and others have utilized for stimulation of MKs (100 ng/ml).

In Vitro Osteoclast-like Cell Formation Models

OC-like cells were generated as previously described (Kacena et al.,2004). In brief, 2×10^6 bone marrow (BM) cells/ml and 20,000 primary calvarial OB/ml were grown in α-MEM supplemented with 10% FCS and 10^{-8} M $1,25(OH)_2D_3$ (Bruzzaniti et al.,2009). The media was changed every other day for 6–8 days (until OC were formed). Once OC formed, the cells were fixed with 2.5% glutaraldehyde in phosphate buffered saline for 30 minutes at room temperature and stained for TRAP. Only $TRAP^+$ multinucleated cells (>3 nuclei) were quantified.

Immunoprecipitation Assays

For immunoprecipitation (IP) analyses, OB were rinsed with ice-cold PBS and lysed in modified RIPA (mRIPA) buffer (50 mM Tris-HCl, pH 7.4), 150 mM NaCl, 5 mM EDTA, 1% NP40, 1% sodium deoxycholate, 0.1% SDS, 50 mM NaF, 1% aprotinin and 0.1mM Na_3VO_4). After a brief sonication, lysed cells were centrifuged at 13,000 rpm for 5 min at 4°C to obtain soluble cell extracts. For immunoprecipitation (IP), approximately 150 μg of lysates were incubated with 3 μg of Anti-TpoR/c-Mpl antibody (Millipore) for 2 h at 4°C. After incubation, 20 μl of Protein G-agarose beads were added to individual tubes for 1 h at 4°C. The beads were washed four times with mRIPA and once with 10 mM Tris-HCl, pH 7.4. The IPs were eluted by boiling for 10 min with 40 μl of 2X Laemmli's sample buffer with β-mercaptoethanol. Immunoblotting was carried out with anti-rabbit secondary antibody (Promega).

Cell Cycle Analysis

WT C57BL/6 and cmp-l −/− calvarial OBs were assessed on days 1, 3, 5, and 7 of culture. Cells were stained with equal volumes of staining buffer (0.1mg/ml propidium iodide + 0.6% Nonidet P40 in PBS) and 2 mg/ml RNase as described previously (Srour et al., 1992). The cells were mixed well and incubated on ice for 30 minutes. Data were collected on a FACS caliber flow cytometer (BDIS) and the percentage of cells in G0/G1 and S/G2+M phases were determined.

Apoptosis Analysis

WT C57BL/6 and cmp-l −/− calvarial OBs were assessed for apoptosis on days 1, 3, 5, and 7 of culture. Cells were washed once in DMEM followed by the addition of Annexin-V conjugated with Aallophycocyanin (APC). Cells were incubated on ice for 15 minutes. Cells were washed and resuspended in DMEM followed by the addition of 10μl of 10ng/ml propidium iodide. Cells were incubated at room temperature for another 10 minutes and data were collected on a FACS caliber flow cytometer.

Alkaline Phosphatase Activity

Alkaline phosphatase activity was determined by the colorimetric conversion of *p*-nitrophenol phosphate to *p*-nitrophenol (Sigma) and normalized to total protein (BCA, Pierce) (Hughes and Aubin, 1998). Briefly, 2 day-old calvarial OB that had been cultured for 14 days were washed 2x with PBS, subsequently lysed with 0.1% (vol/vol) Triton X-100 supplemented with a cocktail of broad-range protease inhibitors (Pierce), subjected to two freeze-thaw cycles, and cleared via centrifugation. Lysates were incubated with 3 mg/ml *p*-nitrophenol phosphate in an alkaline buffer, pH 8.0, (Sigma) for 30 min at 37°C. The reaction was stopped by the addition of 20 mM NaOH and read at 395 nM (GENios Plus, Tecan). The enzymatic activity of alkaline phosphatase was determined by comparison with known *p*-nitrophenol standards (Sigma).

Quantitative Analysis of Calcium Deposition

Calcium deposition was assessed by eluting Alizarin Red S from monolayers of neonatal calvarial OBs grown for 14 days in culture as previously described (Stanford et al.,1995). Briefly, monolayers were washed 2X with PBS, subsequently fixed in ice cold 70% (v/v) ethanol for 1 hr, then washed 2X with water. Monolayers were stained with 40mM Alizarin Red S (pH 4.2) for 10 min (room temperature, shaking), unbound dye was removed by washing with water (5X) and with PBS (1X for 15 minutes, room temperature, shaking). Bound Alizarin Red was eluted by incubating monolayers with 1% (v/v) cetylpyridinium chloride in 10mM sodium phosphate (pH 7.0) for 15 min (room temperature, shaking). Absorbance from aliquots was measured at 562 nm (GENios Plus, Tecan), and Alizarin Red concentrations were calculated from measured standards (Ca/mol of dye in solution).

Quantitative Real-Time PCR

Total RNA was isolated using Trizol Reagent as directed by the manufacturer (Invitrogen Corporation). 1ug of RNA isolated using Trizol Reagent was used to generate cDNA by reverse transcription according to the manufacturer's instructions (First Strand cDNA Synthesis Kit for RT-PCR; Roche Applied Science). Quantitative Real-Time PCR (qRT-PCR) reactions were performed in an ABI Prism 7900HT sequence detection system (Applied Biosystems) using Power SYBR Green PCR Master Mix reagent following the manufacturer's instructions for relative quantification (Applied Biosystems).

For each gene analyzed, a calibration curve was performed and all the oligonucleotides were tested to ensure specificity and sensitivity. For each sample, arbitrary units were obtained using the standard curve and relative mRNA expression of GAPDH was used to normalize the amount of the investigated mRNA transcript. For each target gene, the corresponding

WT sample was used as the calibrator for relative expression. Primer pair sequences used were:

Alkaline phosphatase forward primer:	5’ GCTGATCATTCCCACGTTTT
Alkaline phosphatase reverse primer:	5’ CTGGGCCTGGTAGTTGTTGT
Osteocalcin forward primer:	5’ AAGCAGGAGGGCAATAAGGT
Osteocalcin reverse primer:	5’ TTTGTAGGCGGTCTTCAAGC
Type I collagen forward primer:	5’ CAGGGAAGCCTCTTTCTCCT
Type I collagen reverse primer:	5’ ACGTCCTGGTGAAGTTGGTC
GAPDH forward primer:	5’ CGTGGGGCTGCCCAGAACAT
GAPDH reverse primer:	5’ TCTCCAGGCGGCACGTCAGA
MCSF forward primer:	5’ CCCATATTGCGACACCGAA
MCSF reverse primer:	5’ AAGCAGTAACTGAGCAACGGG
OPG forward primer:	5’ CCGAGTGTGTGAGTGTGAGG
OPG reverse primer	5’ TGCAAACTGTGTTTTGCTCTG
RANKL forward primer:	5’ CATTTGCACACCTCACCATC
RANKL reverse primer:	5’ TCCGTTGCTTAACGTCATGT
EphB2 forward primer:	5’ GATGGTACATCCCCCATCAG
EphB2 reverse primer:	5’ ACGCACCGAGAACTTCATCT
EphB4 forward primer:	5’ CAACTGGATGAGAGCGAGAG
EphB4 reverse primer:	5’ GAGGCAGAGAACTGCAATGA

Statistics

Unless otherwise stated, all data are presented as the Mean ± 1 SD. All experiments were performed at least three times with duplicate or triplicate samples in each experiment. For in vivo studies, the sample size is presented in the corresponding figure legends. Student’s t-test were performed when only two groups were compared. As male and female mouse bones exhibited virtually identical properties, for ease of reporting and to increase the sample size, data from male and female mice were combined for all of the in vivo data analysis. One-way factorial analyses of variances with LSD were used to make multiple group comparisons.

Two-way factorial analyses of variances were used to determine significant main effect contribution in cell co-culture groups, with BM genotype and OB genotype being the independent variables, as well as significant interaction effect between these independent variables. All analyses were performed with the Statistical Package for Social Sciences (IBM SPSS 19; SPSS Inc., Armonk, NY) software and were two tailed with a level of significance set at 0.05.

RESULTS

Trabecular Bone Phenotype of 20 Week-Old C-Mpl−/− Mice

Bones were assessed from male and female c-Mpl−/− and WT mice at 20 weeks. It should be noted that no significant differences were observed in body weights between C57BL/6

and c-Mpl−/− mice (25.8±3.1g vs. 24.1±2.9g, respectively). μCT and static histomorphometry data (trabecular bone) are reported in Table 1. As detailed in Table 1 and illustrated in Figure 1, unexpectedly, bone volume/total volume (BV/TV) was elevated 2.2 fold in c-Mpl−/− mice compared to WT controls as measured by static histomorphometry ($p=0.005$) and 3.4 fold in c-Mpl−/− mice compared to WT controls as measured by μCT ($p<0.001$). C-Mpl−/− femurs exhibited a significant increase in trabecular number (Tb.N, 3.8 fold increase, $p<0.001$) with a concomitant decrease in trabecular spacing (Tb.Sp, 1.8 fold decrease, $p<0.001$) compared to WT controls as measured by μCT. No difference was detected in trabecular thickness (Tb.Th). Of interest, the structural model index or SMI, measured by μCT, was 2.00±0.005 for c-Mpl−/− femurs and 2.69±0.05 for WT control femurs and ($p<0.001$). As an SMI of 3 signifies a more rod-like bone architecture whereas an SMI of 0 signifies a more plate-like structure, c-Mpl deficiency resulted in a more plate-like trabecular architecture.

As shown in Table 1 and Figure 1, examination of static bone histomorphometry parameters illustrated a significant increase in both the number of OBs/tissue area (N.Ob/TAR, 1.6 fold increase, $p=0.05$) and the number of OCs/tissue area (N.Oc/TAR, 2 fold increase, $p=0.003$) from the distal femur of the c-Mpl−/− mice when compared to the WT controls. This finding is not surprising given that OBs and OCs are typically coupled. Thus, it is not unusual to observe a significant increase in both OB and OC numbers. Dynamic bone histomorphometric analyses revealed no significant differences for the distal femur between c-Mpl−/− and WT with respect to bone formation rate/total volume (BFR/TV) or mineral apposition rate (MAR). These data, combined with the bone volume data from μCT and static histomorphometry, suggest c-Mpl−/− mice to have increased numbers of OBs that are similarly active/functional to that of WT mice. However, the increased number of OBs formed more total trabecular bone. As OC numbers were also elevated in c-Mpl−/− mice c-Mpl deficiency produced a high bone mass phenotype, appearing by five months of age, as a result of a high turnover state; similar to what was observed in growing mice.

Anthropometrics, Cortical Bone, Biomechanical and Biomaterial Properties

Anthropometrics and cortical bone histomorphometry are reported in Table 2. Biomechanical and biomaterial property data are reported in Tables 2 and 3. With respect to femoral geometry, no significant differences were detected between c-Mpl−/− and WT mice for femoral length, mid-shaft width (medial to lateral), or mid-shaft height (ventral to dorsal). Consistent with the mid-shaft width and height, polar moment of inertia, calculated via μCT, also revealed no significant difference between c-Mpl−/−and WT femurs. Next, static and dynamic bone histomorphometric data was collected on cross-sectional femur specimens at the mid-shaft. As would be expected based on the gross femur width and height measurements, the cross-sectional area (CSA) was not different between WT and c-Mpl−/− femurs (1.72±0.04 vs. 1.74±0.05, $p=0.8$) as assed by μCT. However, the bone area (BA) was significantly higher in WT femurs compared to c-Mpl−/− femurs (0.86±0.05 vs. 0.72±0.02, $p=0.005$). As might be predicted based on the similar CSA, no difference in periosteal bone formation rate was detected. The increased BA observed in WT mice is likely due to the increased endocortical bone formation rate observed compared to c-Mpl−/− mice ($p=0.03$). With a similar outer geometry but a striking increase in bone area, it would

be predicted that the WT bones would be stronger and stiffer than c-Mpl−/− bones. Specifically, the WT femurs were 18.6% stronger than c-Mpl femurs ($p<0.001$) as determined by examining the peak load. Similarly, the WT femurs were 15.0% stiffer than c-Mpl femurs ($p=0.02$).

C-Mpl is expressed on both Osteoblast and Osteoclast Lineage Cells

Since global deficiency of c-Mpl resulted in a high bone mass phenotype by 5 months of age with changes in both OB and OC parameters observed in vivo, we investigated possible mechanisms leading to this phenotype. First, we determined whether cells of the OB lineage express c-Mpl. As shown in Figure 2A, immunoprecipitation studies demonstrated the expression of c-Mpl in MKs (positive control) and in WT OBs, but not in c-Mpl−/− OBs (negative control). With respect to expression in OC lineage cells, we recently reported that primary bone marrow macrophages (OC progenitors) as well as two OC-like cell lines (RAW264.7 and a PAX5 Spleen Cell Line generated by M. Horowitz) all expressed c-Mpl albeit at lower levels than that observed in MKs (Bethel et al.,2015).

C-Mpl Negatively Regulates Osteoblast Proliferation

To begin to understand the role of c-Mpl expression in OB function, we next sought to determine whether c-Mpl expression affected OB number or cell cycle regulation. To accomplish this, equal numbers of WT and c-Mpl−/− OBs were cultured and assessed every other day (days 1, 3, 5 and 7) for the total number of viable OBs (trypan blue exclusion) produced in culture as well as cell cycle status. As demonstrated in Figure 2, c-Mpl−/− OB cultures produced significantly more cells than their WT counterparts (Figure 2B) and c-Mpl −/− OBs entered active phases of cell cycle at a higher rate than WT OBs (Figure 2C). Of interest, we also cultured OBs in the presence or absence of TPO (kindly provided by Genentech). Supplementation with 100 ng/ml of TPO did not have an effect on total number of OB progeny or their cell cycle. Finally, we also assessed apoptosis by examining the expression of Annexin V. In all cases, less than 2% of the OBs were Annexin V positive, suggesting that apoptosis did not alter proliferation or cell cycle status of OBs in culture.

C-Mpl Expression Does Not Affect Osteoblast Differentiation In Vitro

To understand the effects of c-Mpl expression and signaling on OB differentiation, we examined the following 4 groups of cells: WT OB, WT OB + TPO, c-Mpl−/− OB, and c-Mpl−/− OB + TPO. Cells were cultured under osteogenic conditions as detailed above. As shown in Figures 2D and 2E, we assessed alkaline phosphatase activity and measured bound calcium as a functional measure of mineralization after 14 days. No significant differences were detected between WT and c-Mpl−/− OBs. Furthermore, the addition of 100 ng/ml of TPO did not have a notable effect on WT or c-Mpl−/− OBs.

To further examine the effects of c-Mpl expression in OB differentiation we cultured WT and c-Mpl−/− OBs under osteogenic conditions as above and on day 14 examined mRNA expression of the following genes: alkaline phosphatase, type I collagen, and osteocalcin. As illustrated in Figure 2F, no significant differences in mRNA expression of these genes were observed between WT and c-Mpl−/− OBs.

The Effects of c-Mpl Expression on Osteoclasts

We recently demonstrated that TPO significantly enhanced osteoclastogenesis when bone marrow marcophages (BMMs) were used as a source of OC progenitors, and that fewer OCs were generated from c-Mpl−/− BMMs as compared to those generated from WT BMMs (Taylor et al.,2008). As fewer OCs were generated from c-Mpl−/− BMMs in vitro but higher numbers of OCs were observed in c-Mpl−/− mice in vivo, and because we found that OBs also express c-Mpl, we sought to determine whether c-Mpl−/− OBs promote osteoclastogenesis. To accomplish this, we performed mix-and-match experiments in which OCs were generated by co-culturing of OB and BM supplemented with PGE_2 and Vitamin D_3. Specifically, WT or c-Mpl−/− OBs were co-cultured with BM generated from WT or c-Mpl−/− mice. TRAP+ multinucleated (≥3 nuclei) cells from the 4 experimental groups were analyzed for three parameters: OC number, average nuclei/OC, and average OC surface area. As shown in Figure 3, significant main effect differences were found for both OB and BM genotype with respect to OC number (Figure 3A), number of nuclei/OC (Figure 3B), and OC surface area (Figure 3C). Specifically, c-Mpl−/− OBs supported osteoclastogenesis better than WT OBs, while WT BM cells supported osteoclastogenesis more effectively than c-Mpl−/− BM cells. Notably, a significant interaction was observed between c-Mpl−/− OB genotype and WT BM genotype with increased OC surface area (Figure 3) and increased OC nuclei number (Figure 3B), but not for total OC number (Figure 3A). Finally, as detailed above, our previous independent studies culturing BMMs in the presence of M-CSF and RANKL confirmed co-culture statistical analyses showing that WT BM cells better support osteoclastogenesis than c-Mpl−/− BM cells (Taylor et al.,2008).

C-Mpl Expression Does Not Affect M-CSF, OPG, RANKL, Eph B2, or Eph B4 expression in Osteoblasts

To further understand the mechanism by which expression of c-Mpl on OBs regulates osteoclastogenesis we cultured WT OBs and c-Mpl−/− OBs under osteogenic conditions and examined mRNA expression of the following genes: RANKL, OPG, and M-CSF. As shown in Figure 4, no significant differences were detected suggesting that c-Mpl expression on OBs does not affect OB expression of these known regulators of osteoclastogenesis. The EphrinB2-EphB2/B4 signaling pathway has also been implicated in OB-mediated osteoclastogenesis. Thus, we also determined whether c-Mpl expression altered OB-specific expression of EphB2 or EphB4. No significant differences were detected (Figure 4). Although c-Mpl−/− OBs were able to better support osteoclastogenesis than their WT counterpart, the exact mechanism for this enhanced support remains to be determined.

DISCUSSION

C-Mpl is a member of the type I cytokine receptor family. The receptor along with its ligand, TPO, were first proposed to play a role in megakaryopoiesis when experiments showed that antisense oligonucleotides to c-Mpl reduced MK colony formation (Methia et al.,1993). Upon binding to c-Mpl, TPO has been shown to promote the proliferation and differentiation of MK progenitor cells (Broudy et al.,1995; Kaushansky et al.,1994). The roles of TPO and c-Mpl were further clarified when a mouse model deficient in the gene for TPO exhibited a greater than 80% decrease in MK and platelet numbers (de Sauvage et al.,1996). In their

original study of c-Mpl−/− mice, Gurney et al. noted a marked decrease in MK number, but found no change in the number of mature red blood cells, white blood cells, neutrophils, or eosinophils. The role of TPO and c-Mpl in other hematopoietic lineages was later elucidated. Solar et al found that c-Mpl is expressed in early hematopoietic cells and that TPO is able to activate quiescent progenitors (Solar et al.,1998). This is consistent with the observation that c-Mpl−/− and TPO−/− mice display diminished levels of erythroid, myeloid, and multipotential progenitor cells (Carver-Moore et al.,1996). Indeed, subsequent studies by Carver-Moore et al. showed a significant decrease in all hematopoietic progenitors, including myeloid lineage cells. As OCs are known descendents of myeloid progenitors, it would be understandable if OCs were altered in the c-Mpl deficient mice. Furthermore, our laboratory recently showed that OC progenitors express c-Mpl, that stimulation of OC progenitors with TPO enhances OC formation in vitro, and that binding of TPO to c-Mpl is required for TPO to enhance OC formation in vitro (Taylor et al.,2008). Thus, like MK lineage cells, OC numbers may be expected to be decreased in c-Mpl−/− mice, in part because with the loss of c-Mpl, the ability of TPO to enhance osteoclastogenesis would be largely suppressed and because of the defect observed in myeloid lineage cells. Interestingly, as detailed in Table 1, OC number was significantly higher in c-Mpl−/− mice compared to WT controls. These in vivo findings along with in vitro studies are discussed in further detail below.

As mentioned above, we have demonstrated that increased levels of bone marrow MKs can promote bone formation (Kacena et al.,2005; Kacena et al.,2004). In light of c-Mpl's role in megakaryopoiesis and osteoclastogenesis, we aimed to further understand the c-Mpl−/− bone phenotype. Perry et al previously examined the bone phenotype of 12 week-old c-Mpl deficient mice (Perry et al.,2007). However, we have previously found that the high bone mass phenotype observed in mice with upregulated numbers of MKs (e.g. GATA-1 and NF-E2 deficient mice) was not present until approximately 4 months of age (personal observation MAK and (Kacena et al.,2004; Kacena et al.,2005)). Therefore, here we have examined the bone phenotype of 20 week-old c-Mpl−/− and WT control mice.

Although Perry et al observed no difference in bone phenotype in 12 week-old mice, they predicted a decrease would be observed based on a reduction in the number of MKs (Perry et al.,2007). We report 20-week-old c-Mpl−/− mice to have a high bone mass phenotype (~2–3 fold increase) compared to WT controls. Examining biomechanical properties, femurs from WT mice are stronger and stiffer than those of c-Mpl−/− mice. Of importance, using static and dynamic bone histomorphometry we demonstrated that c-Mpl−/− mice had increased numbers of OBs (N.Ob/TAR), although OB activity appeared unchanged (BFR and MAR). In addition, OC number (N.Oc/TAR) was significantly elevated with c-Mpl deficiency. These findings, in combination with the increased number of OBs and high bone mass phenotype, suggest that c-Mpl deficiency results in a high bone turnover state with a net gain in bone volume.

How this could occur in light of previous postulations that MKs stimulate OB number and bone formation requires some historical background as well as new data. While establishing the role of c-Mpl in MKs and primitive hematopoietic cells, early papers speculated that the receptor is mainly restricted to hematopoietic lineages (Alexander et al.,1996; Mignotte et

al.,1994; de Sauvage et al.,1998). To our knowledge, c-Mpl has never been identified in mesenchymal lineage cells. We present the new observation that c-Mpl is expressed in cells of the OB lineage (Figure 2) in addition to our previous finding that c-Mpl is expressed in OC progenitors (Bethel et al.,2015). With respect to OB lineage cells, c-Mpl−/− OB cultures contained significantly more OBs over a 7 day time period and a larger percentage of cultured c-Mpl−/− OBs were in active phases of the cell cycle between days 3 and 7 compared to WT OBs (Figure 2). Despite significant effects on OB proliferation, our data show no significant difference in differentiation between c-Mpl−/− and WT OBs, as assessed by functional alkaline phosphatase and mineralization assays, and mRNA expression of alkaline phosphatase, type I collagen, and osteocalcin as markers of OB differentiation. Thus, our in vitro data demonstrate that the loss of c-Mpl expression increases OB proliferation, yet does not appear to affect OB differentiation, which is consistent with an increase in OB number but no change in BFR in vivo.

With respect to in vitro osteoclastogenesis we found OC progenitors express c-Mpl (Bethel et al.,2015), WT BM cells respond to OB mediated regulation of osteoclastogenesis to a higher degree than c-Mpl−/− BM cells (Figure 3), and c-Mpl−/− OBs supported osteoclastogenesis better than WT OBs (Figure 3). Next, in an attempt to further understand how c-Mpl deficient OBs better support osteoclastogenesis, we examined OB expression of known regulators of osteoclastogenesis (Figure 4). As no differences were detected in the RANKL/OPG/MCSF or EphrinB2-EphB2/B4 axes, these data suggest that c-Mpl−/− OBs promote osteoclastogenesis through yet an unidentified pathway(s).

In summation, global deficiency of c-Mpl results in a high bone mass phenotype that develops with age. Complex interactions between MKs, OBs, OCs, TPO signaling, and c-Mpl expression in OB and OC progenitors regulate skeletal homeostasis. Figure 5 presents a model summarizing our current understanding of these complex regulations based on our present findings and previously published data. The multiple and varied direct and indirect effects of TPO, c-Mpl, and MKs must be teased out to fully understand their impact on skeletal homeostasis. Use of tissue specific knockout and tissue specific overexpressing mice will be important in clarifying these issues and determining whether therapies targeting MKs and/or TPO/c-Mpl may prove beneficial for treatment of bone loss disorders such as osteoporosis.

Acknowledgments

This work was supported by the Undergraduate Summer Research Program for Prospective Physician-Scientists and Physician-Engineers at Indiana University School of Medicine (TEM), the Diversity Scholars Research Program (TEM), Life-Health Sciences Internships Program (TEM, JTB), the Ronald E. McNair Post-Baccalaureate Achievement Program (JTB), the Medical Student Affairs Summer Research Program in Academic Medicine at Indiana University School of Medicine (SMB), the Department of Orthopaedic Surgery, Indiana University School of Medicine (MAK), the Center of Excellence in Molecular Hematology funded in part by NIH/NIDDK P30 DK090948, the Indiana - Clinical and Translational Sciences Institute funded in part by NIH grant UL1TR001108, and by NIH/NIAMS grants R01 AR060863 (MAK) and R01 AR060332 (MAK, AB, TEM). We would like to thank Genentech and Drs. Fredrick de Sauvage and Wei Tong for providing the c-Mpl−/− mice. Finally, we would like to thank the operators of the Indiana University Melvin and Bren Simon Cancer Center Flow Cytometry Resource Facility (FCRF) for their technical help and support. The FCRF is partially funded by P30 CA082709. The content in this manuscript is solely the responsibility of the authors and does not necessarily represent the official views of the NIH.

REFERENCES

Alexander WS, Maurer AB, Novak U, Harrison-Smith M. Tyrosine-599 of the c-Mpl receptor is required for Shc phosphorylation and the induction of cellular differentiation. EMBO J. 1996; 15:6531–6540. [PubMed: 8978680]

Bethel M, Barnes CL, Taylor AF, Cheng YH, Chitteti BR, Horowitz MC, Bruzzaniti A, Srour EF, Kacena MA. A Novel Role for Thrombopoietin in Regulating Osteoclast Development in Humans and Mice. J Cell Physiol. 2015

Broudy VC, Lin NL, Kaushansky K. Thrombopoietin (c-mpl ligand) acts synergistically with erythropoietin, stem cell factor, and interleukin-11 to enhance murine megakaryocyte colony growth and increases megakaryocyte ploidy in vitro. Blood. 1995; 85:1719–1726. [PubMed: 7535585]

Bruzzaniti A, Neff L, Sandoval A, Du L, Horne WC, Baron R. Dynamin reduces Pyk2 Y402 phosphorylation and SRC binding in osteoclasts. Mol Cell Biol. 2009; 29:3644–3656. [PubMed: 19380485]

Carver-Moore K, Broxmeyer HE, Luoh SM, Cooper S, Peng J, Burstein SA, Moore MW, de Sauvage FJ. Low levels of erythroid and myeloid progenitors in thrombopoietin-and c-mpl-deficient mice. Blood. 1996; 88:803–808. [PubMed: 8704234]

Cheng YH, Hooker RA, Nguyen K, Gerard-O'Riley R, Waning DL, Chitteti BR, Meijome TE, Chua HL, Plett AP, Orschell CM, Srour EF, Mayo LD, Pavalko FM, Bruzzaniti A, Kacena MA. Pyk2 regulates megakaryocyte-induced increases in osteoblast number and bone formation. J Bone Miner Res. 2013; 28:1434–1445. [PubMed: 23362087]

Cheng YH, Streicher DA, Waning DL, Chitteti BR, Gerard-O'Riley R, Horowitz MC, Bidwell JP, Pavalko FM, Srour EF, Mayo LD, Kacena MA. Signaling pathways involved in megakaryocyte-mediated proliferation of osteoblast lineage cells. J Cell Physiol. 2015; 230:578–586. [PubMed: 25160801]

Ciovacco WA, Cheng YH, Horowitz MC, Kacena MA. Immature and mature megakaryocytes enhance osteoblast proliferation and inhibit osteoclast formation. J Cell Biochem. 2010; 109:774–781. [PubMed: 20052670]

Ciovacco WA, Goldberg CG, Taylor AF, Lemieux JM, Horowitz MC, Donahue HJ, Kacena MA. The role of gap junctions in megakaryocyte-mediated osteoblast proliferation and differentiation. Bone. 2009; 44:80–86. [PubMed: 18848655]

de Sauvage FJ, Villeval JL, Shivdasani RA. Regulation of megakaryocytopoiesis and platelet production: Lessons from animal models. 1998; 131:496.

de Sauvage FJ, Carver-Moore K, Luoh SM, Ryan A, Dowd M, Eaton DL, Moore MW. Physiological regulation of early and late stages of megakaryocytopoiesis by thrombopoietin. J Exp Med. 1996; 183:651–656. [PubMed: 8627177]

de Sauvage FJ, Hass PE, Spencer SD, Malloy BE, Gurney AL, Spencer SA, Darbonne WC, Henzel WJ, Wong SC, Kuang WJ. Stimulation of megakaryocytopoiesis and thrombopoiesis by the c-Mpl ligand. Nature. 1994; 369:533–538. [PubMed: 8202154]

Feher A, Koivunemi A, Koivunemi M, Fuchs RK, Burr DB, Phipps RJ, Reinwald S, Allen MR. Bisphosphonates do not inhibit periosteal bone formation in estrogen deficient animals and allow enhanced bone modeling in response to mechanical loading. Bone. 2010; 46:203–207. [PubMed: 19857619]

Gurney AL, Carver-Moore K, de Sauvage FJ, Moore MW. Thrombocytopenia in c-mpl-deficient mice. Science. 1994; 265:1445–1447. [PubMed: 8073287]

Horowitz MC, Fields A, DeMeo D, Qian HY, Bothwell AL, Trepman E. Expression and regulation of Ly-6 differentiation antigens by murine osteoblasts. Endocrinology. 1994; 135:1032–1043. [PubMed: 7520861]

Hughes FJ, Aubin JE. Culture of Cells of the Osteoblast Lineage. 1998:1–49.

Jilka RL, Cohn DV. Role of phosphodiesterase in the parathormone-stimulated adenosine 3',5'-monophosphate response in bone cell populations enriched in osteoclasts and osteoblasts. Endocrinology. 1981; 109:743–747. [PubMed: 6167435]

Kacena MA, Eleniste PP, Cheng YH, Huang S, Shivanna M, Meijome TE, Mayo LD, Bruzzaniti A. Megakaryocytes regulate expression of Pyk2 isoforms and caspase-mediated cleavage of actin in osteoblasts. J Biol Chem. 2012; 287:17257–17268. [PubMed: 22447931]

Kacena MA, Gundberg CM, Nelson T, Horowitz MC. Loss of the transcription factor p45 NF-E2 results in a developmental arrest of megakaryocyte differentiation and the onset of a high bone mass phenotype. Bone. 2005; 36:215–223. [PubMed: 15780947]

Kacena MA, Shivdasani RA, Wilson K, Xi Y, Troiano N, Nazarian A, Gundberg CM, Bouxsein ML, Lorenzo JA, Horowitz MC. Megakaryocyte-osteoblast interaction revealed in mice deficient in transcription factors GATA-1 and NF-E2. J Bone Miner Res. 2004; 19:652–660. [PubMed: 15005853]

Kaushansky K, Lok S, Holly RD, Broudy VC, Lin N, Bailey MC, Forstrom JW, Buddle MM, Oort PJ, Hagen FS. Promotion of megakaryocyte progenitor expansion and differentiation by the c-Mpl ligand thrombopoietin. Nature. 1994; 369:568–571. [PubMed: 8202159]

Lemieux JM, Horowitz MC, Kacena MA. Involvement of integrins alpha(3)beta(1) and alpha(5)beta(1) and glycoprotein IIb in megakaryocyte-induced osteoblast proliferation. J Cell Biochem. 2010; 109:927–932. [PubMed: 20052668]

Meijome TE, Hooker RA, Cheng YH, Walker W, Horowitz MC, Fuchs RK, Kacena MA. GATA-1 deficiency rescues trabecular but not cortical bone in OPG deficient mice. J Cell Physiol. 2015; 230:783–790. [PubMed: 25205203]

Methia N, Louache F, Vainchenker W, Wendling F. Oligodeoxynucleotides antisense to the proto-oncogene c-mpl specifically inhibit in vitro megakaryocytopoiesis. Blood. 1993; 82:1395–1401. [PubMed: 7689867]

Miao D, Murant S, Scutt N, Genever P, Scutt A. Megakaryocyte-bone marrow stromal cell aggregates demonstrate increased colony formation and alkaline phosphatase expression in vitro. Tissue Eng. 2004; 10:807–817. [PubMed: 15265298]

Mignotte V, Vigon I, Boucher de Crevecoeur E, Romeo PH, Lemarchandel V, Chretien S. Structure and transcription of the human c-mpl gene (MPL). Genomics. 1994; 20:5–12. [PubMed: 8020956]

Perry MJ, Redding KA, Alexander WS, Tobias JH. Mice Rendered Severely Deficient in Megakaryocytes through Targeted Gene Deletion of the Thrombopoietin Receptor c-Mpl Have a Normal Skeletal Phenotype. Calcif Tissue Int. 2007; 81:224–231. [PubMed: 17674074]

Shivdasani RA, Fielder P, Keller GA, Orkin SH, de Sauvage FJ. Regulation of the serum concentration of thrombopoietin in thrombocytopenic NF-E2 knockout mice. Blood. 1997; 90:1821–1827. [PubMed: 9292514]

Shivdasani RA, Rosenblatt MF, Zucker-Franklin D, Jackson CW, Hunt P, Saris CJ, Orkin SH. Transcription factor NF-E2 is required for platelet formation independent of the actions of thrombopoietin/MGDF in megakaryocyte development. Cell. 1995; 81:695–704. [PubMed: 7774011]

Simmons DJ, Kent GN, Jilka RL, Scott DM, Fallon M, Cohn DV. Formation of bone by isolated, cultured osteoblasts in millipore diffusion chambers. Calcif Tissue Int. 1982; 34:291–294. [PubMed: 6809292]

Solar GP, Kerr WG, Zeigler FC, Hess D, Donahue C, de Sauvage FJ, Eaton DL. Role of c-mpl in early hematopoiesis. Blood. 1998; 92:4–10. [PubMed: 9639492]

Srour EF, Brandt JE, Leemhuis T, Ballas CB, Hoffman R. Relationship between cytokine-dependent cell cycle progression and MHC class II antigen expression by human CD34+ HLA-DR- bone marrow cells. J Immunol. 1992; 148:815–820. [PubMed: 1370518]

Stanford CM, Jacobson PA, Eanes ED, Lembke LA, Midura RJ. Rapidly forming apatitic mineral in an osteoblastic cell line (UMR 106-01 BSP). J Biol Chem. 1995; 270:9420–9428. [PubMed: 7721867]

Taylor AF, Barnes CLT, Horowitz MC, Kacena MA. A Novel Role for Thrombopoietin in Regulating Osteoclast Development. JBMR. 2008; 23:SU104.

Tong W, Lodish HF. Lnk inhibits Tpo-mpl signaling and Tpo-mediated megakaryocytopoiesis. J Exp Med. 2004; 200:569–580. [PubMed: 15337790]

Villeval JL, Cohen-Solal K, Tulliez M, Giraudier S, Guichard J, Burstein SA, Cramer EM, Vainchenker W, Wendling F. High thrombopoietin production by hematopoietic cells induces a fatal myeloproliferative syndrome in mice. Blood. 1997; 90:4369–4383. [PubMed: 9373248]

Warden SJ, Nelson IR, Fuchs RK, Bliziotes MM, Turner CH. Serotonin (5-hydroxytryptamine) transporter inhibition causes bone loss in adult mice independently of estrogen deficiency. Menopause. 2008; 15:1176–1183. [PubMed: 18725867]

Weatherholt AM, Fuchs RK, Warden SJ. Cortical and trabecular bone adaptation to incremental load magnitudes using the mouse tibial axial compression loading model. Bone. 2013; 52:372–379. [PubMed: 23111313]

Wong GL, Cohn DV. Target cells in bone for parathormone and calcitonin are different: enrichment for each cell type by sequential digestion of mouse calvaria and selective adhesion to polymeric surfaces. Proc Natl Acad Sci U S A. 1975; 72:3167–3171. [PubMed: 171656]

Yan XQ, Lacey D, Hill D, Chen Y, Fletcher F, Hawley RG, McNiece IK. A model of myelofibrosis and osteosclerosis in mice induced by overexpressing thrombopoietin (mpl ligand): reversal of disease by bone marrow transplantation. Blood. 1996; 88:402–409. [PubMed: 8695786]

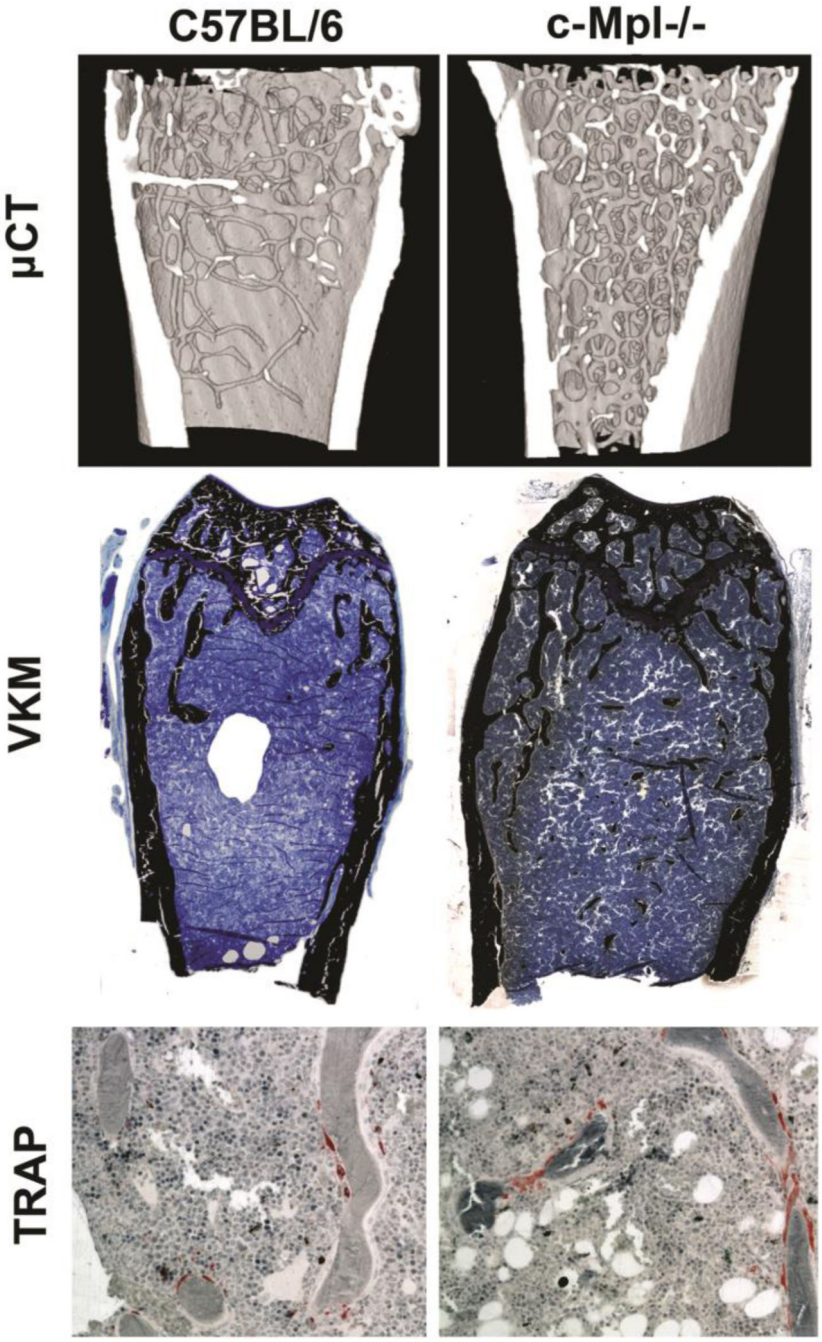

Figure 1.

Representative images of distal femurs from 20 week-old WT and c-Mpl−/− mice. **A**) µCT reconstructions show the high bone mass phenotype in c-Mpl−/− mice compared to WT controls. **B**) Histological sections stained with Von Kossa show the significant increase in mineralized bone matrix in c-Mpl−/− femurs compared to that observed in WT femurs (original magnification 5X). **C**) TRAP staining illustrates the significant increase in OCs in c-Mpl−/− mice compared to WT controls (original magnification 20X).

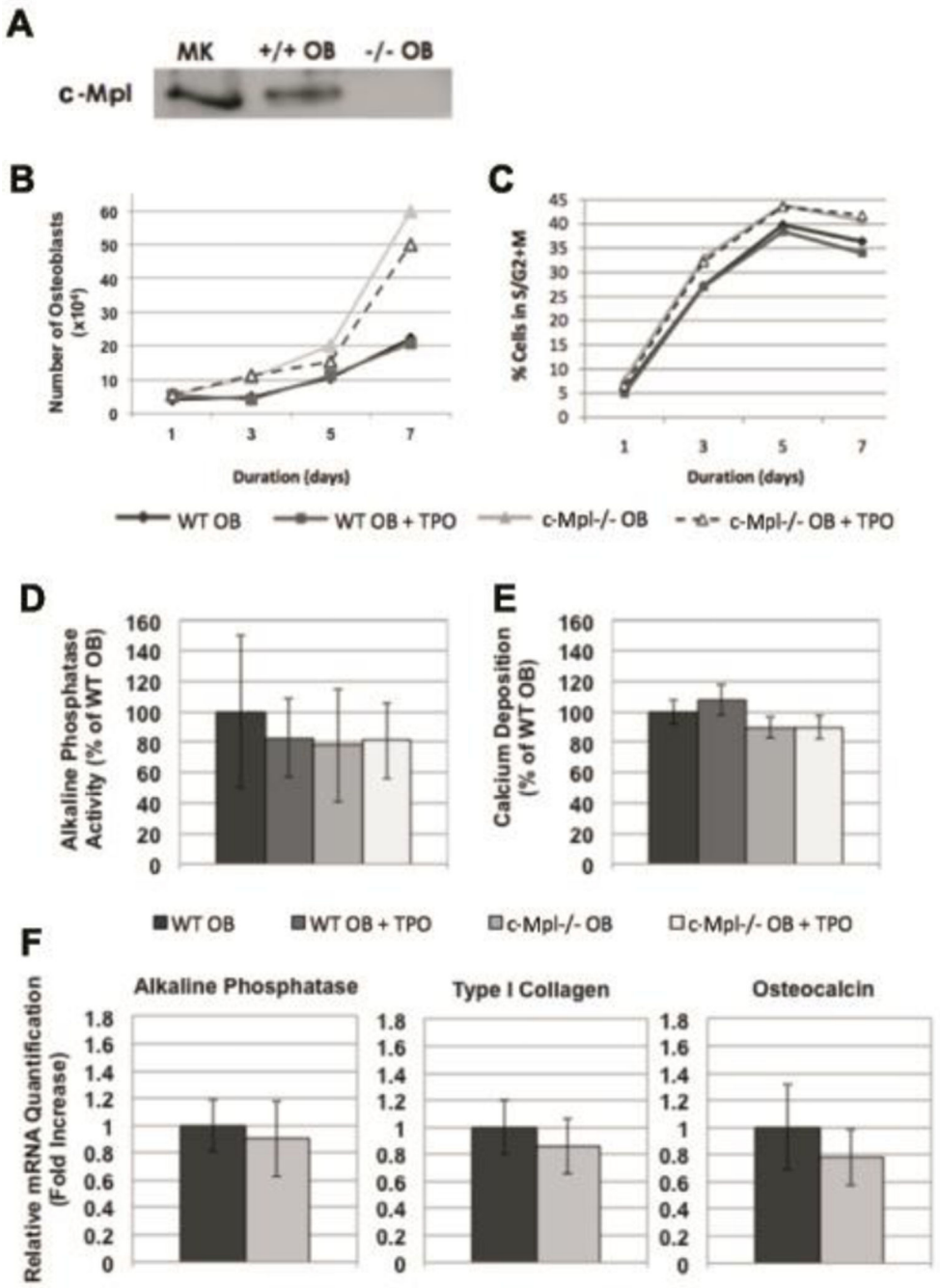

Figure 2.

A) Neonatal calvarial OB lineage cells express c-Mpl as shown by immunoprecipitation of protein lysates from 2 day WT and c-Mpl−/− calvarial OBs and MKs, probed with antibodies raised against c-Mpl, shows that WT OBs express c-Mpl. **B–F)** Proliferation and differentiation of WT and c-Mpl−/− OBs. **B&C)** WT and c-Mpl−/− OBs were cultured and OB number **(B)** and cell cycle status **(C)** was assessed every other day by counting the number of cells excluding trypan blue and by staining OBs with propidium iodide, respectively. Annexin V expression was also determined. In all cases, less than 2% of the

OBs were Annexin V positive, suggesting that apoptosis was not detected. Data shown in Figure **B** reveal that the c-Mpl−/− OB cultures have more cells than do their WT counterparts. Data in Figure **C** illustrates that the c-Mpl−/− OBs enter active phases of cell cycle at a higher rate than WT OBs. These data suggest that the loss of c-Mpl most likely alters the rate at which c-Mpl−/− OBs enter S-G2M and therefore increases the total number of cells. **D–F)** To analyze the role of c-Mpl in OB differentiation, two day calvarial OBs were generated from WT and c-Mpl−/− mice. OBs were cultured under osteogenic conditions (ascorbic acid and and β-glycerophosphate supplementation) for 14 days in the presence or absence of TPO (100ng/ml) and alkaline phosphatase activity **(D)** and bound calcium as a marker of mineralization was measured **(E). F)** Real-time PCR was used to determine mRNA expression of alkaline phosphatase, type I collagen, and osteocalcin. No significant differences were detected suggesting that c-Mpl expression does not affect OB differentiation or expression of the genes examined.

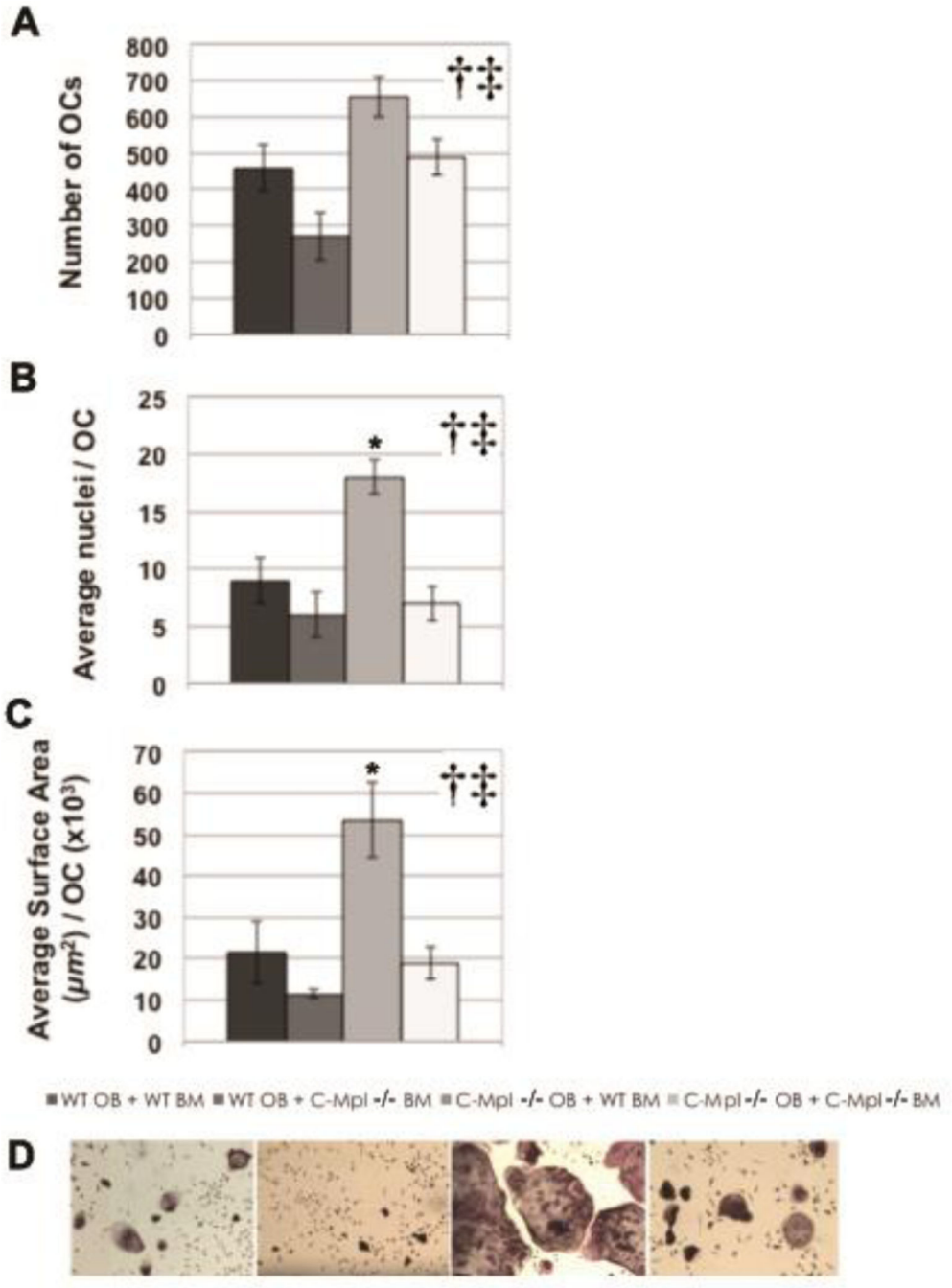

Figure 3.

Histomorphometric analysis of OCs generated by co-culture of WT and c-Mpl−/− OBs with WT and c-Mpl−/− bone marrow (BM) supplemented with PGE2 and Vitamin D3 **(A–C)**. Representative micrographs (original magnification 40X) from each of the 4 experimental groups are shown **(D)**. Once OCs were visible (~7 days for co-cultures), cells were fixed and stained for tartrate resistant acid phosphatase (TRAP), and the TRAP+ multinucleated (≥3 nuclei) cells from the 4 experimental groups were analyzed as follows: 1) OC number **(A)**; 2) Average nuclei/OC **(B)**; and 3) Average OC surface area **(C)**. Significant main effect

differences were found for both OB genotype and BM genotype for OC number, number of nuclei/OC, and OC surface area. Specifically c-Mpl−/− OBs better support osteoclastogenesis than do WT OBs, while WT BM better supports osteoclastogenesis than does c-Mpl−/− BM. Importantly, a significant interaction was observed between OB genotype and BM genotype for OC surface area and nuclei number, but not for total OC number. *Indicates significant interaction was found between OB genotype and BM genotype. †Indicates a significant main effect for OB genotype. ‡Indicates a significant main effect for BM genotype.

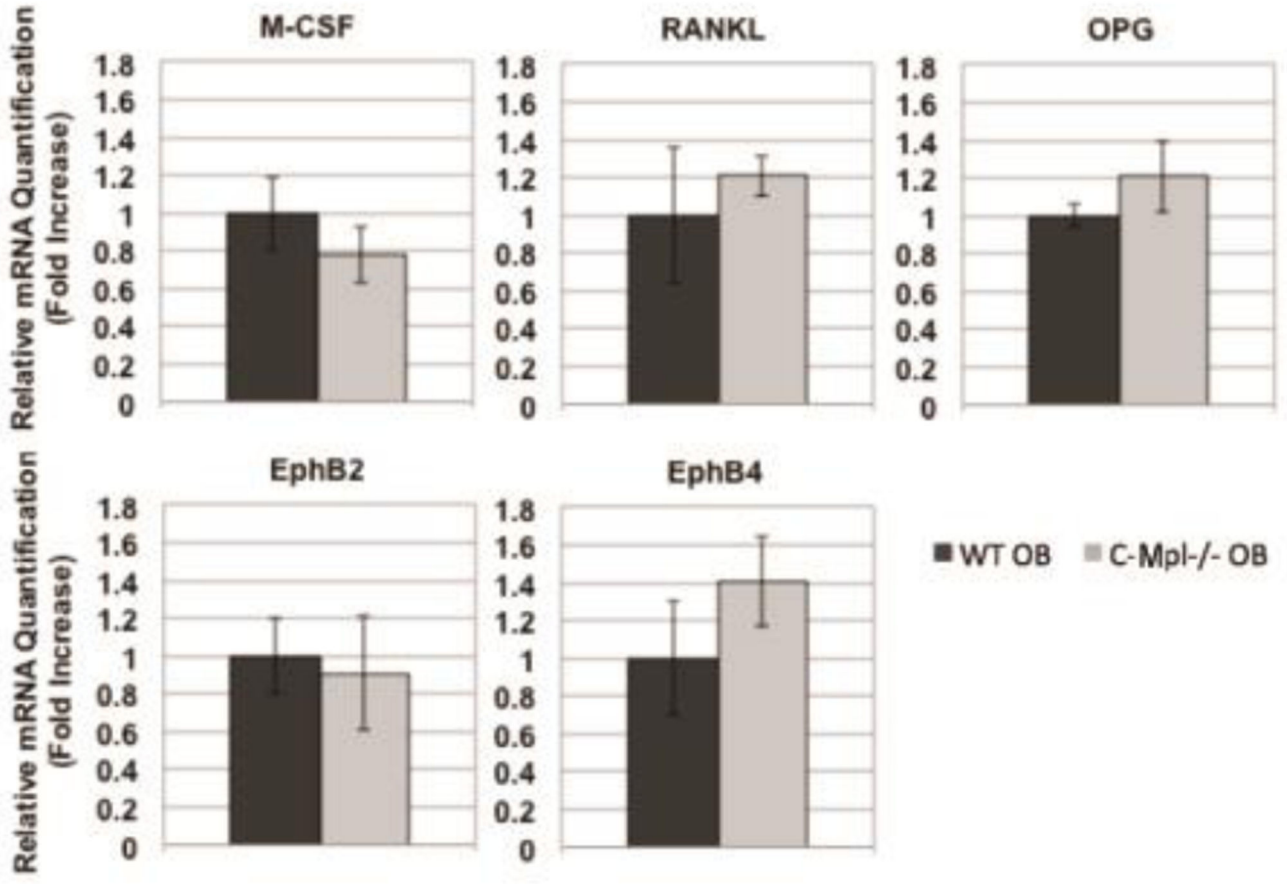

Figure 4.

mRNA expression in WT and c-Mpl−/− OBs. OBs were cultured under osteogenic conditions as before for 7 days. Real-time PCR was used to determine mRNA expression of M-CSF, OPG, RANKL, Eph B2, and Eph B4. GAPDH was used to normalize the amount of the investigated transcript. No significant differences were detected suggesting that c-Mpl expression does not affect OB expression of these known regulators of osteoclastogenesis.

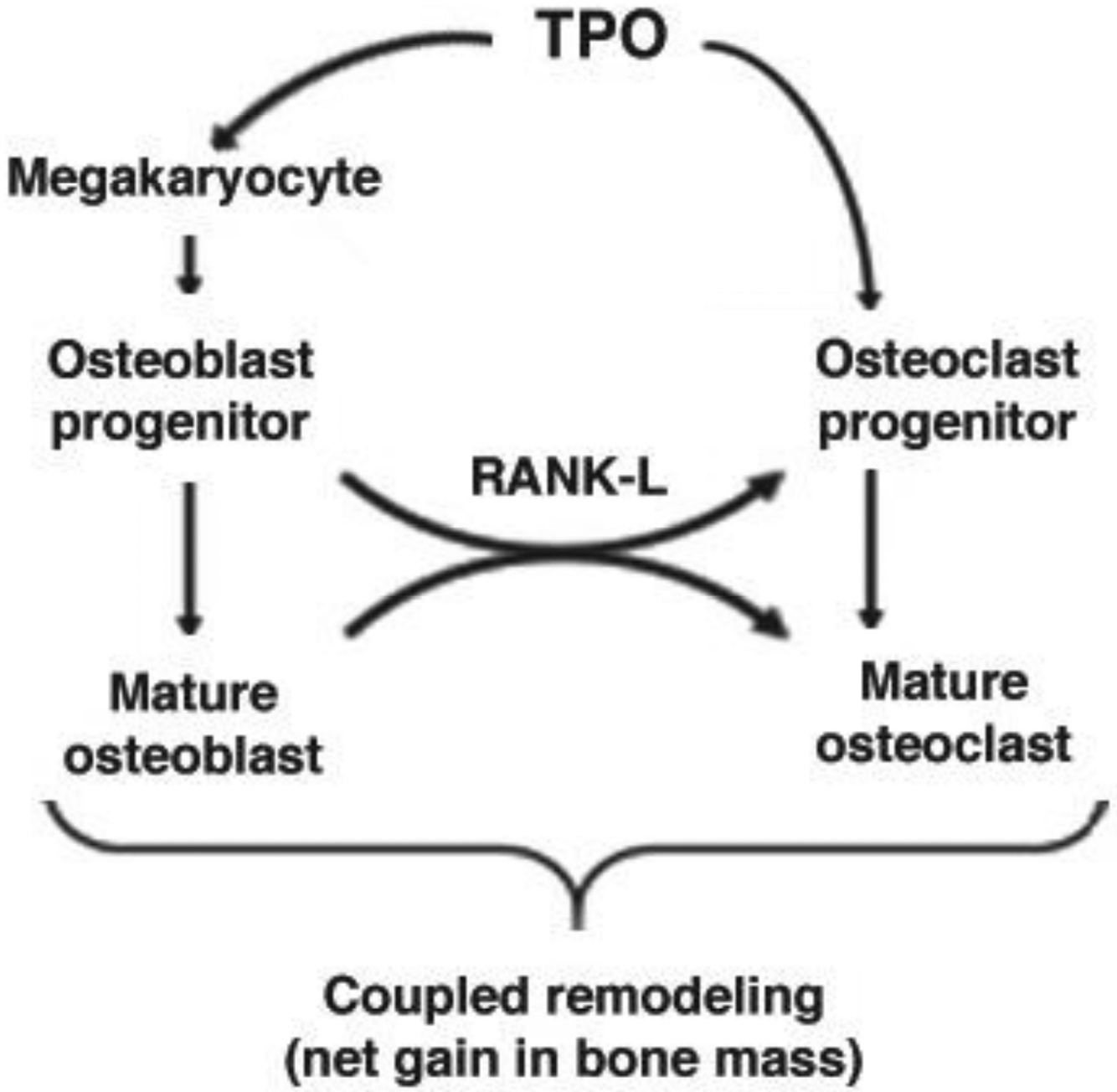

Figure 5.

Working model depicting the direct and indirect effects of TPO/c-Mpl on skeletal homeostasis. In the bone marrow cavity, TPO binds to its receptor c-Mpl on MK/MK progenitors and activation of c-Mpl signaling results in proliferation and differentiation of MKs. MKs enhance OB proliferation by a direct cell-cell contact mechanism. With increased numbers of OBs there is also a net increase in RANKL expression which enhances OC differentiation/activation. At the same time, TPO binds to its receptor c-Mpl on OC progenitors, stimulating a significant increase in mature OC number. However, increased numbers of MKs also inhibit OC formation. Together these actions result in coupled

remodeling in WT mice and a net gain in bone mass in TPO overexpressing mice. With c-Mpl deficiency the opposite is observed with respect to TPO-mediated effects (e.g. effects of TPO on MKs and OC progenitors and associated downstream effects). However, an important difference is noted; C-Mpl−/− OBs proliferate more than do their WT counterpart in vitro and in vivo. Additionally, c-Mpl−/− OBs promote osteoclastogenesis by a yet undetermined mechanism. Combined c-Mpl deficiency results in a high turnover state with a net gain in bone mass.

Table 1

Trabecular bone; MicroCT analysis of distal femurs and static histomorphometric analysis, 20-week old c-Mpl−/− and WT mice

		MicroCT						Histology				
Mice	**n**	**BV/TV (%)**	**SMI**	**Tb.Th (mm)**	**Tb.N (1/mm)**	**Tb.Sp (mm)**	**n**	**BV/TV (%)**	**N.Ob/ TAR**	**N.Oc/ TAR**	**BFR/TV ($\mu m^2/\mu m^3$/year)**	**MAR (μm/day)**
C57BL/6 (WT)	38	3.6 ± 0.3	2.69 ± 0.05	0.053 ± 0.002	0.69 ± 0.05	0.34 ±0 .01	11	3.9 ±0 .8	59 ± 13	29 ± 4	317 ± 43	1.7 ±0 .2
c-Mpl−/−	27	12.4 ± 0.6 *	2.00 ± 0.05 *	0.048 ± 0.001	2.6 ± 0.1 *	0.19 ±0 .01 *	10	8.4 ± 1.1 *	97 ± 13 *	58 ± 8 *	354 ± 22	1.9 ±0 .1

BV/TV, bone volume/total volume; SMI, structure model index; Tb.Th, trabecular thickness; Tb.N, trabecular number; Tb.Sp, trabecular separation; BV/TV, bone volume/total volume; N.Ob/TAR, number of osteoblasts/tissue area; N.Oc/TAR, number of osteoclasts/tissue area; BFR/TV, bone formation rate/tissue volume; MAR, mineral apposition rate.

Results are presented as mean ± SEM;

* Indicates significant difference compared to WT ($p<0.05$)

Table 2

Anthropometrics, cortical bone histomorphometry properties, 20-week old c-Mpl−/− and WT mice

	Anthropometrics				Cortical Bone Histomorphometry				
Mice	**n**	**Length (μm)**	**Width (μm)**	**Height (μm)**	**n**	**CSA (μm^2)**	**BA (μm^2)**	**Periosteal BFR ($\mu m^2/\mu m^3$/day)**	**Endocortical BFR ($\mu m^2/\mu m^3$/day)**
C57BL/6 (WT)	37	15.3 ± 0.1	1.74 ± 0.03	1.29 ± 0.02	19	1.72 ±0 .04	0.86 ± 0.05	17 ± 4	53 ± 2
c-Mpl−/−	26	15.0 ± 0 .1	1.76 ± 0 .03	1.26 ± 0.02	10	1.74 ±0 .05	0.72 ±0 .02 *	17 ± 4	33 ± 5 *

Length, distal to proximal femur length; Width, medial to lateral femur width; Height, ventral to dorsal femur height; CSA, cross-sectional area; BA, bone area; Periosteal BFR, periosteal bone formation rate; Endocortical BFR, endocortical bone formation rate.

Results are presented as mean ± SEM;

* Indicates significant difference compared with gender matched WT ($p<0.05$)

Table 3

Biomechanical and biomaterial properties, 20-week old c-Mpl−/− and WT mice

Biomechanical and Biomaterial properties						
Mice	**n**	**Polar MOI (mm^4)**	**Modulus (MPa)**	**Load at Peak (N)**	**Stiffness (N/mm)**	**Ultimate Failure (MPa)**
C57BL/6 (WT)	37	0.36 ± 0.01	42797 ± 1673	23.0 ± 0.4	123 ± 4	249 ± 6
c-Mpl−/−	26	0.40 ± 0.02	35095 ± 2766 *	19.4 ± 0.4 *	107 ± 6 *	198 ± 6 *

Polar MOI, polar moment of inertia.

Results are presented as mean ± SEM;

* Indicates significant difference compared with gender matched WT ($p<0.05$);